

## Warm arctic continents during the Palaeocene–Eocene thermal maximum

Johan W.H. Weijers<sup>a,1</sup>, Stefan Schouten<sup>a</sup>, Appy Sluijs<sup>b</sup>,  
Henk Brinkhuis<sup>b</sup>, Jaap S. Sinninghe Damsté<sup>a,c,\*</sup>

<sup>a</sup> Royal Netherlands Institute for Sea Research (NIOZ), Department of Marine Biogeochemistry and Toxicology,  
P.O. Box 59, 1790 AB Den Burg — Texel, The Netherlands

<sup>b</sup> Palaeoecology, Institute of Environmental Biology, Utrecht University, Laboratory of Palaeobotany and Palynology,  
Budapestlaan 4, 3584 CD Utrecht, The Netherlands

<sup>c</sup> Department of Earth Sciences, Utrecht University, Budapestlaan 4, 3584 CD, Utrecht, The Netherlands

Received 6 February 2007; received in revised form 12 June 2007; accepted 22 June 2007

Available online 17 July 2007

Editor: M.L. Delaney

### Abstract

The Palaeocene–Eocene Thermal Maximum (PETM; ~55.5 Ma) is a geologically relatively brief episode of extreme warmth. Both deep and surface ocean temperatures increased by up to 5 °C in equatorial waters and up to 8 °C in mid and high latitude waters. From the continents, the annual mean air temperature response during the PETM is still largely unknown, mainly due to a lack of quantitative temperature proxies and sufficient suitable, continuous high resolution records. Recently, a new proxy for continental temperature reconstructions has been proposed, based on the distribution of membrane lipids of bacteria in present-day soils [J.W.H. Weijers, S. Schouten, J.C. van den Donker, E.C. Hopmans, J.S. Sinninghe Damsté (2007) *Environmental controls on bacterial tetraether membrane lipid distribution in soils, Geochimica et Cosmochimica Acta* 71, 703–713] and shown to reconstruct annual mean air temperature. In this study we applied this new proxy in an attempt to reconstruct the air temperature in high latitude continental areas during the PETM by analysis of a marine sedimentary sequence obtained from the Lomonosov Ridge in the central Arctic Ocean (Integrated Ocean Drilling Program Expedition 302, Site 004, Hole A). The results indicate a warming of ~8 °C above background values of ~17 °C. This warming is coincident with a similar rise in sea surface temperatures documented earlier. Our results thus further confirm the warm conditions in the Arctic, and point to a strongly reduced latitudinal temperature gradient during the PETM.

© 2007 Elsevier B.V. All rights reserved.

**Keywords:** Palaeocene–Eocene thermal maximum; continental air temperature; latitudinal temperature gradient; Arctic Ocean; branched tetraether membrane lipid; Integrated Ocean Drilling Program Expedition 302

\* Corresponding author. Tel.: +31 222 369550; fax: +31 222 319674.

E-mail addresses: [jweijers@nioz.nl](mailto:jweijers@nioz.nl), [johan.weijers@bristol.ac.uk](mailto:johan.weijers@bristol.ac.uk) (J.W.H. Weijers), [schouten@nioz.nl](mailto:schouten@nioz.nl) (S. Schouten), [a.sluijs@uu.nl](mailto:a.sluijs@uu.nl) (A. Sluijs), [h.brinkhuis@uu.nl](mailto:h.brinkhuis@uu.nl) (H. Brinkhuis), [damste@nioz.nl](mailto:damste@nioz.nl) (J.S. Sinninghe Damsté).

<sup>1</sup> Currently at: Organic Geochemistry Unit, Bristol Biogeochemistry Research Centre, School of Chemistry, University of Bristol, Cantock's Close, Bristol, BS8 1TS, United Kingdom.

## 1. Introduction

Superimposed on the already warm climates of the early Cenozoic, the Palaeocene–Eocene Thermal Maximum (PETM) at ~55.5 million years ago represents a geologically relatively brief episode (~170 kyr; Sluijs et al., *in press*) of extreme global warming. Sediments deposited during the PETM are also characterized by a strong negative excursion (2.5 to 6 ‰) in the stable carbon isotope ( $\delta^{13}\text{C}$ ) records of carbonates and organic carbon in both the marine and terrestrial realms (e.g., Kennett and Stott, 1991; Koch et al., 1992; Wing et al., 2005; Sluijs et al., 2006; Schouten et al., 2007). This excursion is considered to be associated with the release of massive amounts of  $^{13}\text{C}$ -depleted carbon into the ocean and atmosphere system (e.g., Dickens et al., 1995; Pagani et al., 2006a and references therein; Storey et al., 2007). Biotic responses to the climatic changes during the PETM include rapid floral range changes (Wing et al., 2005), large scale faunal dispersion (Koch et al., 1992; Smith et al., 2006), as well as massive benthic extinctions (Kennett and Stott, 1991) and proliferation of exotic foraminifera (Kelly et al., 1996) and the dinoflagellate taxon ‘Apectodinium’ (e.g., Bujak and Brinkhuis, 1998; Crouch et al., 2001).

During the PETM, the deep oceans warmed globally by 4 to 6 °C (e.g., Kennett and Stott, 1991; Bralower et al., 1995; Tripathi and Elderfield, 2005). Sea surface temperatures (SST) in the tropics showed a warming of up to 5 °C (Bralower et al., 1995; Thomas et al., 1999; Zachos et al., 2003) while stronger warming of 5 to 8 °C has been reported for the mid and high latitude oceans (Kennett and Stott, 1991; Zachos et al., 2003; Sluijs et al., 2006; Zachos et al., 2006). Compared to the marine realm relatively little is known about changes in the annual mean air temperature (MAT) on the continents during the PETM, due to a lack of quantitative temperature proxies in combination with the relative short duration of the PETM. Several qualitative climate reconstructions indicate generally warmer conditions throughout on the continents around the PETM, notably at higher latitudes (e.g., Robert and Kennett, 1994; Markwick, 1998; Francis and Poole, 2002). Based, for example, on leaf margin analysis and oxygen isotope analysis of fossil teeth enamel, a temperature increase of about 5 to 7 °C has been inferred for the PETM in mid latitude North America (Fricke and Wing, 2004; Wing et al., 2005). Unfortunately, however, continuous high resolution records of MAT on the continents are not available for the PETM interval.

Recently, a new method for estimating terrestrial annual MAT has been developed based on the relative

distribution of branched glycerol dialkyl glycerol tetraether (GDGT) membrane lipids derived from bacteria thriving in soils (Weijers et al., 2006, 2007b). The distribution of branched GDGTs in a globally distributed set of modern soils, expressed in the Methylation index of Branched Tetraethers (MBT) and the Cyclisation ratio of Branched Tetraethers (CBT), shows a significant linear correlation with modern annual MAT in the range of –6 to 27 °C (Weijers et al., 2007b). Since these membrane lipids are fluvially transported to the oceans (Hopmans et al., 2004), analysing marine sedimentary records in front of large river outflows potentially provides continuous high resolution records of river basin integrated continental temperature signals. Based on a sediment record from the Congo deep sea fan, for example, Weijers et al. (2007a) were able to reconstruct the change in annual MAT over the last deglaciation for the Congo River basin, covering almost the whole of tropical central Africa. Here, we apply this new method to a sedimentary sequence from the Lomonosov Ridge in the Arctic Ocean covering the PETM interval. During the PETM this site received considerable fluvial terrestrial organic matter input (Sluijs et al., 2006). By analysing the distribution of the soil-derived GDGT lipids in this sediment core we aimed to reconstruct annual MAT for the high latitude Arctic landmass during the PETM. In addition, palynomorph assemblages were analysed in order to constrain the geographic source of the temperature signal in this core.

## 2. Methods

### 2.1. Sample and site description

Marine sediment samples are derived from Integrated Ocean Drilling Program (IODP) Hole 302-4A (~87° 52.00' N; 136° 10.64' E; 1288 m water depth), positioned on the Lomonosov Ridge in the central Arctic Ocean (Fig. 1), recovered during IODP Expedition 302 (or Arctic Coring Expedition; ACEX) in August 2004 (Backman et al., 2006). This marine sedimentary sequence comprises a Palaeogene record containing the PETM interval between 391 and 378 m composite depth (mcd) (Fig. 3). Due to drilling disturbances and incomplete recovery the lower boundary of the PETM interval and the exact stratigraphic position of Core 31X are somewhat problematic (see Sluijs et al., 2006). In total 43 samples have been analysed (see data table in electronic Appendix) with a resolution of about 5 samples per meter, or, for the PETM interval, a time resolution of ca. 1 sample per 5 kyr using a ~170 kyr duration of the PETM (Sluijs et al., *in press*).

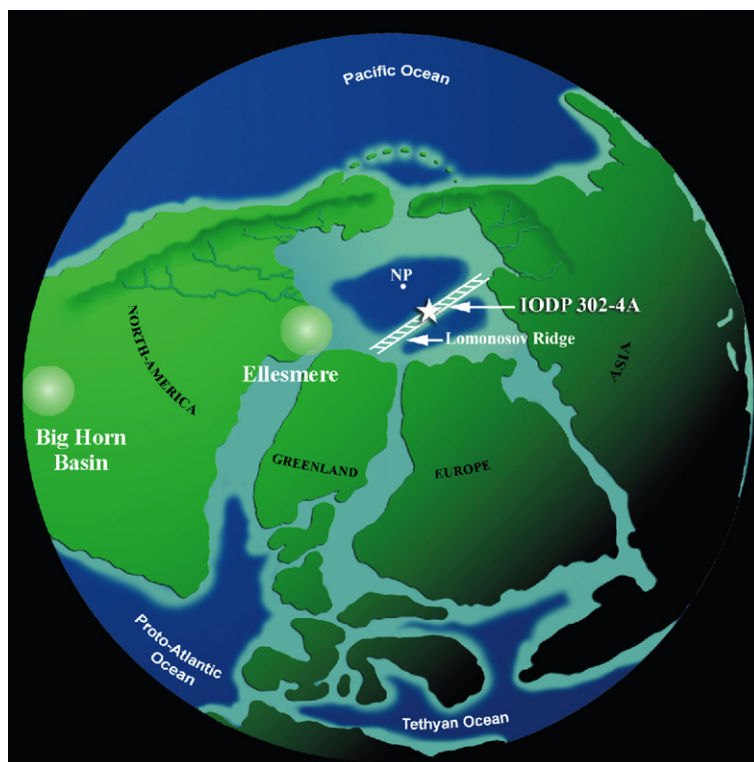


Fig. 1. Location of IODP Hole 302-4A in the palaeogeographical context of the late Palaeocene–early Eocene. Also indicated are the approximate palaeolocations of Ellesmere Island and the Bighorn Basin area, for which temperature estimates around the PETM have been reported (see also Table 1). This figure is modified from Sluijs et al. (2006).

The Lomonosov Ridge represents a part of the Barentsz Shelf that rifted from the Svalbard margin and subsequently drifted away towards the pole where it submerged to its present depth during the Cenozoic (Jokat et al., 1992). During the late Palaeocene, this location was strongly influenced by fresh water input as evident from organic walled dinoflagellate cyst (dinocyst) assemblages and high proportions of terrestrial palynomorphs (Sluijs et al., 2006). The PETM section has been recognized on basis of the concomitant occurrence of a  $\sim 6\%$  negative excursion in  $\delta^{13}\text{C}_{\text{org}}$  values and the occurrence of the dinocyst species *Apectodinium augustum*, which is diagnostic of the PETM (Bujak and Brinkhuis, 1998; Sluijs et al., 2006).

## 2.2. Sample preparation and HPLC/MS analysis

Powdered and freeze dried sediments (1–3 g dry mass) were extracted with an accelerated solvent extractor (Dionex2000), using a dichloromethane (DCM):MeOH 9:1 (v/v) solvent mixture, 3 times for 5 min at a pressure of ca  $7.6 \times 10^6$  Pa and a temperature of 100 °C. The obtained total extracts were rotary evaporated and separated over an activated  $\text{Al}_2\text{O}_3$  column using hexane:DCM 9:1 (v/v)

and DCM:MeOH 1:1 (v/v) solvent mixtures into an apolar and polar fraction, respectively. The polar fraction, containing the branched GDGTs, was dried under a pure  $\text{N}_2$  flow, dissolved ultrasonically in a hexane:propanol 99:1 (v/v) mixture at a concentration of  $2 \text{ mg ml}^{-1}$  and filtered over an  $0.45 \mu\text{m}$  mesh PTFE filter ( $\phi 4 \text{ mm}$ ) prior to HPLC/MS analysis.

High performance liquid chromatography–atmospheric pressure chemical ionization/mass spectrometry (HPLC–APCI/MS) analyses were performed on an Agilent 1100 series/Hewlett–Packard 1100 MSD series machine equipped with auto-injector and HP Chemstation software as described previously (Hopmans et al., 2000) with minor modifications. Injection volume was usually  $10 \mu\text{l}$  and separation of the compounds was achieved in normal phase on a Prevail Cyano column ( $150 \text{ mm} \times 2.1 \text{ mm}$ ;  $3 \mu\text{m}$ ; Alltech). The flow rate of the hexane:propanol 99:1 (v/v) eluent was  $0.2 \text{ ml min}^{-1}$ , isocratically for the first 5 min and thereafter with a linear gradient to 1.8% propanol in 45 min. Analyses were performed in selective ion monitoring mode in order to increase sensitivity and reproducibility. Branched GDGTs were quantified by integrating the area of the  $[\text{M}+\text{H}]^+$  peaks (protonated molecular ion)

and comparing these with an external standard curve prepared with known amounts of the isoprenoid GDGT crenarchaeol. The CBT ratio and MBT index were calculated as follows:

$$\text{CBT} = -\text{Log} \left( \frac{([\text{Ib}] + [\text{IIb}])}{([\text{I}] + [\text{II}])} \right) \quad (1)$$

MBT

$$= \frac{([\text{I}] + [\text{Ib}] + [\text{Ic}])}{([\text{I}] + [\text{Ib}] + [\text{Ic}]) + ([\text{II}] + [\text{IIb}] + [\text{IIc}]) + ([\text{III}] + [\text{IIIb}] + [\text{IIIc}])}. \quad (2)$$

Roman numerals correspond to the GDGT structures drawn in Fig. 2. Annual MAT was then calculated from the CBT and MBT values using the calibration equation given by Weijers et al. (2007b):

$$\text{MBT} = 0.122 + 0.187 * \text{CBT} + 0.020 * \text{MAT} \quad (R^2 = 0.77). \quad (3)$$

Based on duplicate measurement of the whole data series the average standard deviation of the absolute temperature estimates (analytical reproducibility) has been determined at 0.4 °C.

### 2.3. Palynological analysis

Sediments were oven-dried at 60 °C. Samples were treated with 30% HCl and twice with 30% HF for carbonate and silicate removal, respectively. After sieving over a 15- $\mu\text{m}$  nylon mesh sieve, residues were analysed at 500 $\times$  magnification.

## 3. Results and discussion

### 3.1. Temperature estimates based on soil derived branched GDGT lipids

Concentrations of the soil derived branched GDGT membrane lipids are  $\sim 90 \mu\text{g g}^{-1}$  dry weight sediment (dws) during the PETM interval which is higher than the values of 10 and  $60 \mu\text{g g}^{-1}$  dws obtained from the pre- and post-PETM sections of this core, respectively. Based on the rather constant and substantial TOC contents ( $\sim 2\%$ ) in combination with well preserved palynomorphs both within and outside the PETM section, this difference is unlikely to be the result of differences in preservation conditions (Sluijs et al., 2006). Instead, the higher concentrations of branched GDGTs during the PETM might suggest higher productivity of the terrestrial vegetation and/or enhanced river discharge during the PETM, which is consistent with the more

humid conditions at the North Pole at that time (Pagani et al., 2006b). Since terrestrial organic matter input was high, it was possible to determine the degree of cyclisation (CBT) and methylation (MBT) of these terrestrial derived branched GDGTs in the sediments of this core and hence to reconstruct the continental annual MAT. The geographic source of the branched GDGTs in the core from the Lomonosov Ridge determines the continental area for which the MAT is reconstructed. Spreading along the Gakkel Ridge had already separated the Lomonosov Ridge from the Siberian Shelf by the latest Palaeocene (Jokat et al., 1992). Palaeoenvironmental and tectonic studies have indicated that the coring site itself was only shallowly submerged at the PETM (Backman et al., 2006; Sluijs et al., 2006). Hence, it could be argued that the bulk of the terrestrial material was derived from parts of the Lomonosov Ridge close to the coring site that were still above sea level. This hypothesis is supported by palynological data. In upper

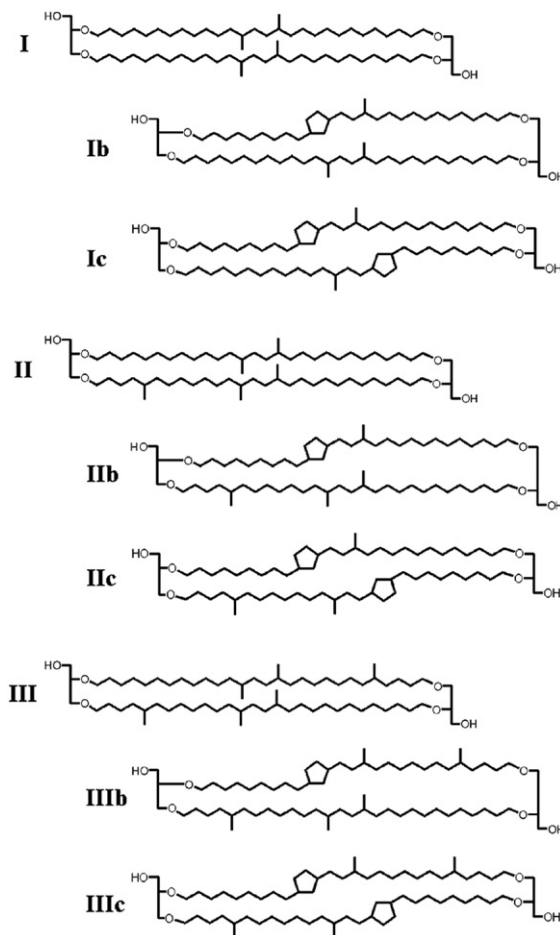


Fig. 2. Chemical structures of the branched glycerol dialkyl glycerol tetraether (GDGT) membrane lipids of soil bacteria used in this study.

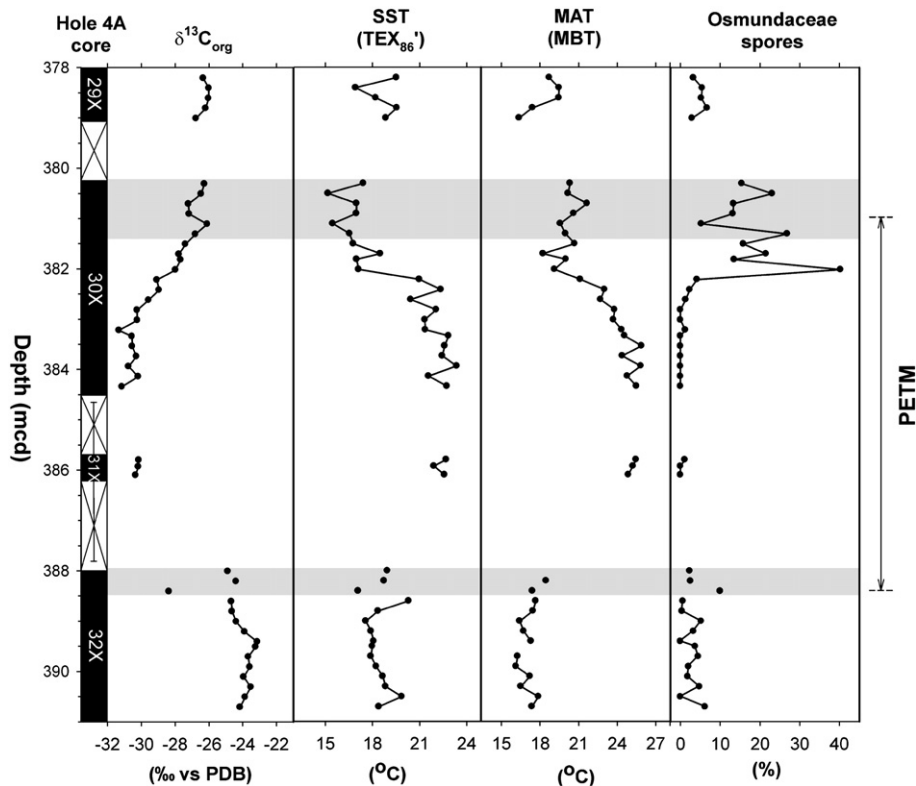


Fig. 3. Annual mean air temperature (MAT) across the PETM for the Lomonosov Ridge in the Arctic Ocean. (a)  $\delta^{13}\text{C}_{\text{org}}$  of total organic carbon (Sluijs et al., 2006), (b)  $\text{TEX}_{86}'$  derived sea surface temperature (SST) (Sluijs et al., 2006), (c) MAT derived from branched GDGT membrane lipids in IODP Hole 302-4A, (d) percentage of Osmundaceae spores (as percentage of the total sum of terrestrial palynomorphs). Error bars in the core recovery column indicate the uncertain stratigraphic position of Core 31X, see also Sluijs et al. (2006). Grey bars indicate intervals affected by drilling disturbance. mcd. = meters composite depth; MBT = Methylation index of Branched Tetraethers.

Palaeocene and lower Eocene strata, spores produced by the fern family Osmundaceae are consistently present and locally abundant (Fig. 3). These spores are very large and cannot have been transported over long distances, and thus the site must have been very close to shore. The consistent occurrence of Osmundaceae spores implies that parts of the Lomonosov Ridge close to the core site were indeed still above sea level and were the source of these Osmundaceae spores and most likely the main portion of the branched GDGTs. The reconstructed MAT is thus thought to represent central Arctic polar conditions. The reconstructed annual MAT shows values of 16 to 18 °C for the latest Palaeocene and increases to values up to 25 °C during the PETM (Fig. 3). Towards the end of the PETM, temperatures drop again to values of around 18 to 20 °C. This transient temperature change parallels the negative  $\delta^{13}\text{C}_{\text{org}}$  excursion and the acme of the subtropical dinoflagellate *Apectodinium augustum* (Sluijs et al., 2006). Higher temperatures occur at the time of lower  $\delta^{13}\text{C}_{\text{org}}$  values and the subsequent cooling mirrors the recovery pattern of  $\delta^{13}\text{C}_{\text{org}}$  (Fig. 3).

Our MAT record for the central Arctic Lomonosov Ridge compares well with the SST reconstruction for the Arctic Ocean at this location by Sluijs et al. (2006). On the basis of the  $\text{TEX}_{86}'$  proxy, their reconstruction shows SSTs of ~18 °C for the latest Palaeocene, >23 °C for the PETM, and a cooling towards ~17 °C at the end of the PETM (Fig. 3). Thus, both proxies indicate a strong climatic warming in the Arctic region during the PETM, and a cooling towards the end of the PETM consistent with the recovery of the  $\delta^{13}\text{C}_{\text{org}}$  signal. Remarkably, the absolute temperatures estimated by both proxies are also similar, particularly so when taking into account uncertainties like the exact temporal origin of the temperature signals in this high latitude area, i.e. annual mean or seasonal temperatures. It has to be emphasised that both organic proxies are based on different compounds and source organisms. Where the  $\text{TEX}_{86}$  SST proxy is based on the membrane lipids of marine Crenarchaeota which are ubiquitous in marine sediments (Schouten et al., 2002), the MBT MAT proxy is based on soil-derived branched GDGT membrane

Table 1  
Overview of Palaeocene–Eocene continental temperature estimates

Time interval	Location	Palaeo Lat.	Method	Temperature	Reference
Early Eocene	Lomonosov Ridge	~75° N	MBT/CBT	~17 °C	This study
	Ellesmere Island Canada	71° N	Crocodile remains	≥14 °C <sup>a</sup>	Markwick (1998)
	Bighorn Basin Wyoming, USA	45° N	Leaf margin analyses	~18 °C <sup>b</sup>	Wing et al. (2000)
PETM	Lomonosov Ridge	~75° N	MBT/CBT	~25 °C	This study
	Coastal continent Antarctica	65° S <sup>c</sup>	Clay mineral composition	≥15 °C <sup>d</sup>	Robert and Kennett (1994)
	Bighorn Basin Wyoming, USA	45° N	Leaf margin analyses	~20 °C <sup>b</sup>	Wing et al. (2005)
	Bighorn Basin Wyoming, USA	45° N	δ <sup>18</sup> O composition of fossil teeth	~26 °C	Fricke and Wing (2004)
Late Palaeocene	Lomonosov Ridge	~75° N	MBT/CBT	~19 °C	This study
	Bighorn Basin Wyoming, USA	45° N	Leaf margin analyses	~15 °C <sup>b</sup>	Wing et al. (2000)

<sup>a</sup> Minimum mean annual air temperature required for the presence of crocodiles.

<sup>b</sup> Underestimate; see text for discussion.

<sup>c</sup> This represents the latitude of the Ocean Drilling Program Site 690B at Maud Rise; Antarctic coastline is at ~70° S.

<sup>d</sup> Formation temperature of kaolinite and thus minimum soil temperature; the overall clay mineral composition is indicative of sub-tropical conditions.

lipids which are only detected in trace amounts in open marine settings and thus indicative for a predominant terrestrial source (Hopmans et al., 2004). Both proxies are, moreover, differently calibrated and hence totally independent. The similarity between both records, therefore, emphasises once again that temperature is exerting the main control on GDGT lipid distributions. In addition, the similar absolute estimates for both land and sea surface temperatures are a first and strong independent confirmation that temperatures in the Arctic during the PETM were indeed extremely high compared to the present-day situation.

There are, however, a number of uncertainties associated with the temperature reconstruction presented here. The original calibration between the MBT index and annual MAT and soil pH (Eq. (3)) shows some scatter, mainly due to the heterogeneity of soils and uncertainties in MAT estimates (see discussion in Weijers et al., 2007b). Overall, this scatter gives rise to a standard error of estimate of the absolute temperature estimate of ca. 5 °C and, thus, absolute MAT estimates should be interpreted with care. Nevertheless, if the MBT proxy is applied at near coastal sites, preferably nearby a river mouth, the obtained temperature values will represent a signal integrated over a whole river basin, thereby averaging out part of the scatter present in the calibration set (cf. Weijers et al., 2007a). Other uncertainties include the origin of the MBT signal, which must be known, i.e. the extent and topography of the drainage basin, and the impact of seasonality. The topography of the Lomonosov Ridge is not yet known in detail. Based on the relatively small landmass, however, it is assumed that this ridge did not contain extensive highlands and the obtained temperature record is, therefore, expected to represent a lowland temperature signal. Concerning seasonality, a bias towards summer

temperatures might be expected mainly because the season of maximum growth likely occurred during the polar day (summer) season, but also because the estimated MAT is similar to the TEX<sub>86</sub>' SST for which a summer bias was already invoked (Sluijs et al., 2006). Branched GDGT membrane lipids, however, are produced by ostensibly non-phototrophic bacteria thriving in the anoxic parts of soils and peat bogs (Weijers et al., 2006). Therefore, these bacteria are expected not to be affected by polar night/day conditions. As, in addition, frost conditions are suggested to be absent during the PETM (Bice et al., 1996; Tripati et al., 2001; Jahren, 2007), especially on this ridge surrounded by warm Arctic waters (Sluijs et al., 2006), there is no *a priori* reason why the MBT proxy is recording summer temperatures alone. Other possibilities, like changing nutrient conditions in soils during polar night conditions cannot be excluded but remain purely speculative. Despite these uncertainties, the relatively smooth trend of our MAT record and the parallel evolution with the TEX<sub>86</sub>' and δ<sup>13</sup>C<sub>org</sub> records strongly suggest that air temperatures at the high latitude Arctic Lomonosov Ridge were high during the PETM and increased by up to 8 °C above background values.

### 3.2. Comparison to other Palaeocene–Eocene temperature estimates

As noted above, and in contrast to the marine realm, terrestrial temperature estimates for the PETM interval are very scarce. For high latitude regions only two semi-quantitative temperature estimates, i.e. minimum estimates, are available (Robert and Kennett, 1994; Markwick, 1998, see Table 1). In addition to the minimum temperature provided by the clay mineral assemblage derived from coastal Antarctica, its composition during

the PETM interval compares to that found in modern tropical to subtropical Atlantic sediments, which even suggests subtropical conditions on coastal Antarctica during the PETM (Robert and Kennett, 1994). Absolute estimates of annual MAT for the PETM are only derived from the Big Horn Basin area, Wyoming USA, which was located at a palaeolatitude of  $\sim 45^\circ$  N. Temperature estimates based on leaf margin analysis (Wing et al., 2000, 2005) are  $\sim 6^\circ\text{C}$  lower than temperatures derived from oxygen isotope ratio analyses of phosphate in teeth from fossil animals from the same area (Fricke and Wing, 2004) (Table 1). This could be explained by the fact that floras of predominantly wet-soil environments, as used in the Big Horn Basin study, generally show a greater proportion of toothed leaves, resulting in possible temperature underestimates of up to  $10^\circ\text{C}$  (Kowalski and Dilcher, 2003). Considering this possible bias, this implies that subtropical to tropical temperature conditions might have occurred at the mid-latitude North American continent during the PETM. Remarkably, these mid-latitude PETM temperature estimates are, even if taking into account the uncertainties accompanying the different methods, at most similar to the maximum PETM temperatures reconstructed for the central Arctic Lomonosov Ridge and likely not substantially higher. One possible explanation might be that the peak PETM warmth was missed in the Bighorn Basin section due to the relatively poor stratigraphic resolution of the samples. On the other hand, due to the strong seasonal difference at the high latitudes, our Arctic air temperature estimates might indeed represent maximum (summer) estimates. Alternatively, our data are in support of the idea that the latitudinal thermal gradient between the high and mid latitudes was very small during the PETM, a feature which seems to be characteristic of greenhouse climates (e.g., Huber et al., 1995).

### 3.3. Implications

Our record of polar continental PETM air temperatures, in conjunction with the few other available high latitude temperature estimates (Kennett and Stott, 1991; Robert and Kennett, 1994; Sluijs et al., 2006), provide strong indications of subtropical conditions at the Earth's polar regions during the PETM. This has considerable implications for our knowledge of the Earth's climate state under elevated greenhouse gas levels in an ice free world. Several modelling studies have been conducted to simulate the response of Earth's climate to high greenhouse gas levels for the PETM (e.g., Schmidt and Shindell, 2003; Shellito et al., 2003; Renssen et al., 2004; Shellito and Sloan, 2006). In agreement with proxy data

(e.g., Kennett and Stott, 1991), these models show increased warming which is amplified at the high latitudes, i.e. ca.  $5$  to  $8^\circ\text{C}$  (e.g., Renssen et al., 2004). However, the simulated absolute temperatures for the high latitudes are near freezing point (e.g., Shellito et al., 2003; Shellito and Sloan, 2006) and hence considerably lower than the indications from proxy data. Thus, proxy data indicate a latitudinal thermal gradient that is much flatter than simulated by climate models which generally yield gradients of  $\sim 30^\circ\text{C}$  (e.g., Shellito et al., 2003; Shellito and Sloan, 2006).

Apparently, current climate models lack one or more physical mechanisms that are able to warm the polar regions without substantially increasing temperatures in the tropics during the early Cenozoic. Several reasons have been suggested explaining this model-data discrepancy. These include the presence of sea ice in models, a lack of proper boundary conditions like sea surface temperatures and topography, and an increased oceanic and/or atmospheric heat transport during the PETM. None of these, however, can explain the model-data discrepancy (Huber and Sloan, 1999, 2001; Sloan et al., 2001; Caballero and Langen, 2005). Considered to be more plausible feedback mechanisms in reducing the tropic-to-pole temperature gradient during the early Cenozoic in general and PETM in particular are a higher abundance of polar stratospheric clouds (Sloan and Pollard, 1998) and enhanced poleward oceanic heat transport induced by tropical cyclones (Srifer and Huber, 2007).

The seemingly sub-tropical conditions at the poles (Robert and Kennett, 1994; Sluijs et al., 2006 and this study) and conservative temperature estimates in excess of  $33^\circ\text{C}$  for the mid latitudes (Zachos et al., 2006), might imply that temperatures at the equator were as high as  $40^\circ\text{C}$  during the PETM. Published reconstructions of Cretaceous SSTs at low to mid latitudes using the  $\text{TEX}_{86}$ ,  $\delta^{18}\text{O}$  and Mg/Ca proxies (Schouten et al., 2003; Bice et al., 2006; Zachos et al., 2006; Forster et al., 2007) do suggest that tropical sea waters may have indeed been as high as  $40^\circ\text{C}$  in the geological past. Thus, there may have been a latitudinal thermal gradient at the PETM. Nonetheless, it still must have been much smaller than today and, in addition, superimposed on temperatures that were globally substantially higher than currently assumed.

## 4. Conclusions

Using a new organic proxy for reconstructing continental air temperatures, the MBT index, we estimated temperatures for the Lomonosov Ridge in the Arctic

Ocean during the PETM. The reconstructed temperature signal is most likely derived from the Lomonosov Ridge itself, which was partially still above sea level. Air temperatures clearly increased by about 8 °C above already warm background temperatures, a similar amplitude as observed for high latitude sea surface waters. Although the exact temporal origin of the reconstructed temperature signal is somewhat uncertain, the estimated values of 17 °C prior to the PETM and 25 °C during the PETM match well with the reconstructed sea surface temperature for the Arctic Ocean at this time interval. These values confirm a much reduced latitudinal temperature gradient in the PETM greenhouse world compared to the present-day situation.

### Acknowledgements

We thank E. Hopmans for analytical assistance with the HPLC/MS system. This research was supported by the Earth and Life Sciences council of the Netherlands Organisation for Scientific Research (ALW-NWO). This research used samples and data provided by the Integrated Ocean Drilling Program (IODP). IODP is sponsored by the U.S. National Science Foundation (NSF) and participating countries under management of Joint Oceanographic Institutions (JOI) Incorporated. We thank the Netherlands Organization for Scientific Research (NWO) for their continued support of ODP and IODP.

### Appendix A. Supplementary data

Supplementary data associated with this article can be found, in the online version, at [doi:10.1016/j.epsl.2007.06.033](https://doi.org/10.1016/j.epsl.2007.06.033).

### References

- Backman, J., Moran, K., McInroy, D.B., Mayer, L.A., the Expedition 302 Scientists, 2006. Arctic Coring Expedition (ACEX). Proc. IODP 302. [doi:10.2204/iodp.proc.302.2006](https://doi.org/10.2204/iodp.proc.302.2006)-(Integrated Ocean Drilling Program Management International, College Station, Texas, 2006).
- Bice, K.L., Arthur, M.A., Marincovich, L., 1996. Late Paleocene Arctic Ocean shallow-marine temperatures from mollusc stable isotopes. *Paleoceanography* 11, 241–249.
- Bice, K.L., Birgel, D., Meyers, P.A., Dahl, K.A., Hinrichs, K.U., Norris, R.D., 2006. A multiple proxy and model study of Cretaceous upper ocean temperatures and atmospheric CO<sub>2</sub> concentrations. *Paleoceanography* 21. [doi:10.1029/2005PA001203](https://doi.org/10.1029/2005PA001203).
- Bralower, T.J., Zachos, J.C., Thomas, E., Parrow, M., Paull, C.K., Kelly, D.C., Silva, I.P., Sliter, W.v., Lohmann, K.C., 1995. Late Paleocene to Eocene paleoceanography of the equatorial Pacific-Ocean — stable isotopes recorded at Ocean Drilling Program Site-865, Allison-Guyot. *Paleoceanography* 10, 841–865.
- Bujak, J.P., Brinkhuis, H., 1998. Global warming and dinocyst changes across the Paleocene/Eocene Epoch boundary. In: Aubry, M.-P., Lucas, S.G., Berggren, W.A. (Eds.), *Late Paleocene–Early Eocene Climatic and Biotic Events in the Marine and Terrestrial Records*. Columbia University Press, New York, pp. 277–295.
- Caballero, R., Langen, P.L., 2005. The dynamic range of poleward energy transport in an atmospheric general circulation model. *Geophys. Res. Lett.* 32, L02705. [doi:10.1029/2004GL021581](https://doi.org/10.1029/2004GL021581).
- Crouch, E.M., Heilmann-Clausen, C., Brinkhuis, H., Morgans, H.E.G., Rogers, K.M., Egger, H., Schmitz, B., 2001. Global dinoflagellate event associated with the late Paleocene thermal maximum. *Geology* 29, 315–318.
- Dickens, G.R., O'Neil, J.R., Rea, D.K., Owen, R.M., 1995. Dissociation of oceanic methane hydrate as a cause of the carbon isotope excursion at the end of the Paleocene. *Paleoceanography* 10, 965–971.
- Forster, A., Schouten, S., Moriya, K., Wilson, P.A., Sinninghe Damsté, J.S., 2007. Tropical warming and intermittent cooling during the Cenomanian/Turonian Oceanic Anoxic Event (OAE 2): sea surface temperature records from the equatorial Atlantic. *Paleoceanography* 22, PA1219. [doi:10.1029/2006PA001349](https://doi.org/10.1029/2006PA001349).
- Francis, J.E., Poole, I., 2002. Cretaceous and early Tertiary climates of Antarctica: evidence from fossil wood. *Palaeogeogr. Palaeoclimatol. Palaeoecol.* 182, 47–64.
- Fricke, H.C., Wing, S.L., 2004. Oxygen isotope and paleobotanical estimates of temperature and  $\delta^{18}\text{O}$ -latitude gradients over North America during the early Eocene. *Am. J. Sci.* 304, 612–635.
- Hopmans, E.C., Schouten, S., Pancost, R.D., van der Meer, M.T.J., Sinninghe Damsté, J.S., 2000. Analysis of intact tetraether lipids in archaeal cell material and sediments by high performance liquid chromatography/atmospheric pressure chemical ionization mass spectrometry. *Rapid Commun. Mass Spectrom.* 14, 585–589.
- Hopmans, E.C., Weijers, J.W.H., Schefuß, E., Herfort, L., Sinninghe Damsté, J.S., Schouten, S., 2004. A novel proxy for terrestrial organic matter in sediments based on branched and isoprenoid tetraether lipids. *Earth Planet. Sci. Lett.* 224, 107–116.
- Huber, M., Sloan, L.C., 1999. Warm climate transitions: a general circulation modeling study of the Late Paleocene thermal maximum (about 56 Ma). *J. Geophys. Res. Atm.* 104, 16633–16655.
- Huber, M., Sloan, L.C., 2001. Heat transport, deep waters, and thermal gradients: coupled simulation of an Eocene greenhouse climate. *Geophys. Res. Lett.* 28, 3481–3484.
- Huber, B.T., Hodell, D.A., Hamilton, C.P., 1995. Middle–Late Cretaceous climate of the Southern high-latitudes — stable isotopic evidence for minimal equator-to-pole thermal-gradients. *Geol. Soc. Amer. Bull.* 107, 1164–1191.
- Jahren, A.H., 2007. The Arctic forest of the middle Eocene. *Annu. Rev. Earth Planet. Sci.* 35, 509–540.
- Jokat, W., Uenzelmannneben, G., Kristoffersen, Y., Rasmussen, T.M., 1992. Lomonosov Ridge — a double-sided continental-margin. *Geology* 20, 887–890.
- Kelly, D.C., Bralower, T.J., Zachos, J.C., Silva, I.P., Thomas, E., 1996. Rapid diversification of planktonic foraminifera in the tropical Pacific (ODP Site 865) during the late Paleocene thermal maximum. *Geology* 24, 423–426.
- Kennett, J.P., Stott, L.D., 1991. Abrupt deep-sea warming, paleoceanographic changes and benthic extinctions at the end of the Paleocene. *Nature* 353, 225–229.
- Koch, P.L., Zachos, J.C., Gingerich, P.D., 1992. Correlation between isotope records in marine and continental carbon reservoirs near the Paleocene Eocene boundary. *Nature* 358, 319–322.
- Kowalski, E.A., Dilcher, D.L., 2003. Warmer paleotemperatures for terrestrial ecosystems. *Proc. Natl. Acad. Sci. U. S. A.* 100, 167–170.

- Markwick, P.J., 1998. Fossil crocodylians as indicators of Late Cretaceous and Cenozoic climates: implications for using palaeontological data in reconstructing palaeoclimate. *Palaeogeogr. Palaeoclimatol. Palaeoecol.* 137, 205–271.
- Pagani, M., Caldeira, K., Archer, D., Zachos, J.C., 2006a. An ancient carbon mystery. *Science* 314, 1556–1557.
- Pagani, M., Pedentchouk, N., Huber, M., Sluijs, A., Schouten, S., Brinkhuis, H., Sinninghe Damsté, J.S., Dickens, G.R., 2006b. Arctic hydrology during global warming at the Palaeocene/Eocene thermal maximum. *Nature* 442, 671–675.
- Renssen, H., Beets, C.J., Fichetef, T., Goosse, H., Kroon, D., 2004. Modeling the climate response to a massive methane release from gas hydrates. *Paleoceanography* 19. doi:10.1029/2003PA000968.
- Robert, C., Kennett, J.P., 1994. Antarctic subtropical humid episode at the Paleocene–Eocene boundary — clay-mineral evidence. *Geology* 22, 211–214.
- Schmidt, G.A., Shindell, D.T., 2003. Atmospheric composition, radiative forcing, and climate change as a consequence of a massive methane release from gas hydrates. *Paleoceanography* 18. doi:10.1029/2002PA000757.
- Schouten, S., Hopmans, E.C., Schefuß, E., Sinninghe Damsté, J.S., 2002. Distributional variations in marine crenarchaeotal membrane lipids: a new tool for reconstructing ancient sea water temperatures? *Earth Planet. Sci. Lett.* 204, 265–274.
- Schouten, S., Hopmans, E.C., Forster, A., van Breugel, Y., Kuypers, M.M.M., Sinninghe Damsté, J.S., 2003. Extremely high sea-surface temperatures at low latitudes during the middle Cretaceous as revealed by archaeal membrane lipids. *Geology* 31, 1069–1072.
- Schouten, S., Woltering, M., Rijpstra, W.I.C., Sluijs, A., Brinkhuis, H., Sinninghe Damsté, J.S., 2007. The Paleocene–Eocene carbon isotope excursion in higher plant organic matter: differential fractionation of angiosperms and conifers in the Arctic. *Earth Planet. Sci. Lett.* 258, 581–592.
- Shellito, C.J., Sloan, L.C., 2006. Reconstructing a lost Eocene paradise: part I. Simulating the change in global floral distribution at the initial Eocene thermal maximum. *Glob. Planet. Change* 50, 1–17.
- Shellito, C.J., Sloan, L.C., Huber, M., 2003. Climate model sensitivity to atmospheric CO<sub>2</sub> levels in the Early–Middle Paleogene. *Palaeogeogr. Palaeoclimatol. Palaeoecol.* 193, 113–123.
- Sloan, L.C., Pollard, D., 1998. Polar stratospheric clouds: a high latitude warming mechanism in an ancient greenhouse world. *Geophys. Res. Lett.* 25, 3517–3520.
- Sloan, L.C., Huber, M., Crowley, T.J., Sewall, J.O., Baum, S., 2001. Effect of sea surface temperature configuration on model simulations of “equable” climate in the Early Eocene. *Palaeogeogr. Palaeoclimatol. Palaeoecol.* 167, 321–335.
- Sluijs, A., Schouten, S., Pagani, M., Woltering, M., Brinkhuis, H., Sinninghe Damsté, J.S., Dickens, G.R., Huber, M., Reichert, G.J., Stein, R., Matthiessen, J., Lourens, L.J., Pedentchouk, N., Backman, J., Moran, K., 2006. Subtropical Arctic Ocean temperatures during the Palaeocene/Eocene thermal maximum. *Nature* 441, 610–613.
- Sluijs, A., Bowen, G.J., Brinkhuis, H., Lourens, L.J., Thomas, E., in press. The Palaeocene–Eocene thermal maximum super greenhouse: biotic and geochemical signatures, age models and mechanisms of global change. In: Williams, M., Haywood, A., Gregory, J., Schmidt, D.N. (Eds.), *Deep time perspectives on Climate Change*. Geological Society of London, TMS Special Publication, London.
- Smith, T., Rose, K.D., Gingerich, P.D., 2006. Rapid Asia–Europe–North America geographic dispersal of earliest Eocene primate *Teilhardina* during the Paleocene–Eocene Thermal Maximum. *Proc. Natl. Acad. Sci. U. S. A.* 103, 11223–11227.
- Sriver, R.L., Huber, M., 2007. Observational evidence for an ocean heat pump induced by tropical cyclones. *Nature* 447, 577–580.
- Storey, M., Duncan, R.A., Swisher III, C.C., 2007. Paleocene–Eocene Thermal Maximum and the opening of the Northeast Atlantic. *Science* 316, 587–589.
- Thomas, D.J., Bralower, T.J., Zachos, J.C., 1999. New evidence for subtropical warming during the late Paleocene thermal maximum: stable isotopes from Deep Sea Drilling Project Site 527, Walvis Ridge. *Paleoceanography* 14, 561–570.
- Tripathi, A., Elderfield, H., 2005. Deep-sea temperature and circulation changes at the Paleocene–Eocene thermal maximum. *Science* 308, 1894–1898.
- Tripathi, A., Zachos, J., Marincovich, L., Bice, K.L., 2001. Late Paleocene Arctic coastal climate inferred from molluscan stable and radiogenic isotope ratios. *Palaeogeogr. Palaeoclimatol. Palaeoecol.* 170, 101–113.
- Weijers, J.W.H., Schouten, S., Hopmans, E.C., Geenevasen, J.A.J., David, O.R.P., Coleman, J.M., Pancost, R.D., Sinninghe Damsté, J.S., 2006. Membrane lipids of mesophilic anaerobic bacteria thriving in peats have typical archaeal traits. *Environ. Microbiol.* 8, 648–657.
- Weijers, J.W.H., Schefuß, E., Schouten, S., Sinninghe Damsté, J.S., 2007a. Coupled thermal and hydrological evolution of tropical Africa over the last deglaciation. *Science* 315, 1701–1704.
- Weijers, J.W.H., Schouten, S., van den Donker, J.C., Hopmans, E.C., Sinninghe Damsté, J.S., 2007b. Environmental controls on bacterial tetraether membrane lipid distribution in soils. *Geochim. Cosmochim. Acta* 71, 703–713.
- Wing, S.L., Bao, H., Koch, P.L., 2000. An early Eocene cool period? Evidence for continental cooling during the warmest part of the Cenozoic. In: Huber, B.T., MacLeod, K.G., Wing, S.L. (Eds.), *Warm Climates in Earth History*. Cambridge University Press, Cambridge UK, pp. 197–237.
- Wing, S.L., Harrington, G.J., Smith, F.A., Bloch, J.I., Boyer, D.M., Freeman, K.H., 2005. Transient floral change and rapid global warming at the Paleocene–Eocene boundary. *Science* 310, 993–996.
- Zachos, J.C., Wara, M.W., Bohaty, S., Delaney, M.L., Petrizzo, M.R., Brill, A., Bralower, T.J., Premoli-Silva, I., 2003. A transient rise in tropical sea surface temperature during the Paleocene–Eocene Thermal Maximum. *Science* 302, 1551–1554.
- Zachos, J.C., Schouten, S., Bohaty, S., Quattlebaum, T., Sluijs, A., Brinkhuis, H., Gibbs, S.J., Bralower, T.J., 2006. Extreme warming of mid-latitude coastal ocean during the Paleocene–Eocene Thermal Maximum: inferences from TEX86 and isotope data. *Geology* 34, 737–740.